

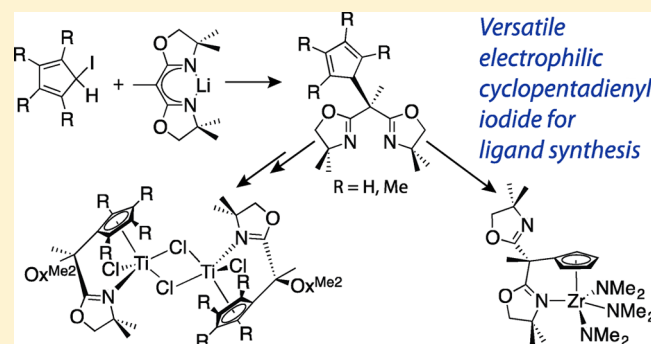
Cyclopentadienyl-bis(oxazoline) Magnesium and Zirconium Complexes in Aminoalkene Hydroaminations

Naresh Eedugurala, Megan Hovey, Hung-An Ho, Barun Jana, Nicole L. Lampland, Arkady Ellern, and Aaron D. Sadow*

U.S. DOE Ames Laboratory and Department of Chemistry, Iowa State University, 1605 Gilman Hall, Ames, Iowa 50011-3111, United States

Supporting Information

ABSTRACT: A new class of cyclopentadiene-bis(oxazoline) compounds and their piano-stool-type organometallic complexes have been prepared as catalysts for hydroamination of aminoalkenes. The two compounds $\text{MeC}(\text{Ox}^{\text{Me}_2})_2\text{C}_5\text{H}_5$ ($\text{Bo}^{\text{M}}\text{CpH}$; Ox^{Me_2} = 4,4-dimethyl-2-oxazoline) and $\text{MeC}(\text{Ox}^{\text{Me}_2})_2\text{C}_5\text{Me}_4\text{H}$ ($\text{Bo}^{\text{M}}\text{Cp}^{\text{tet}}\text{H}$) are synthesized from $\text{C}_5\text{R}_4\text{HI}$ ($\text{R} = \text{H}, \text{Me}$) and $\text{MeC}(\text{Ox}^{\text{Me}_2})_2\text{Li}$. These cyclopentadiene-bis(oxazolines) are converted into ligands that support a variety of metal centers in piano-stool-type geometries, and here we report the preparation of Mg, Tl, Ti, and Zr compounds. $\text{Bo}^{\text{M}}\text{CpH}$ and $\text{Bo}^{\text{M}}\text{Cp}^{\text{tet}}\text{H}$ react with $\text{MgMe}_2(\text{O}_2\text{C}_4\text{H}_8)_2$ to give the magnesium methyl complexes $\{\text{Bo}^{\text{M}}\text{Cp}\}\text{MgMe}$ and $\{\text{Bo}^{\text{M}}\text{Cp}^{\text{tet}}\}\text{MgMe}$. $\text{Bo}^{\text{M}}\text{CpH}$ and $\text{Bo}^{\text{M}}\text{Cp}^{\text{tet}}\text{H}$ are converted to $\text{Bo}^{\text{M}}\text{CpTl}$ and $\text{Bo}^{\text{M}}\text{Cp}^{\text{tet}}\text{Tl}$ by reaction with TlOEt . The thallium derivatives react with $\text{TiCl}_3(\text{THF})_3$ to provide $[\{\text{Bo}^{\text{M}}\text{Cp}\}\text{TiCl}(\mu\text{-Cl})_2]$ and $[\{\text{Bo}^{\text{M}}\text{Cp}^{\text{tet}}\}\text{TiCl}(\mu\text{-Cl})_2]$, the former of which is crystallographically characterized as a dimeric species. $\text{Bo}^{\text{M}}\text{CpH}$ and $\text{Zr}(\text{NMe}_2)_4$ react to eliminate dimethylamine and afford $\{\text{Bo}^{\text{M}}\text{Cp}\}\text{Zr}(\text{NMe}_2)_3$, which is crystallographically characterized as a monomeric four-legged piano-stool compound. $\{\text{Bo}^{\text{M}}\text{Cp}\}\text{Zr}(\text{NMe}_2)_3$, $\{\text{Bo}^{\text{M}}\text{Cp}\}\text{MgMe}$, and $\{\text{Bo}^{\text{M}}\text{Cp}^{\text{tet}}\}\text{MgMe}$ are efficient catalysts for the hydroamination/cyclization of aminoalkenes under mild conditions.

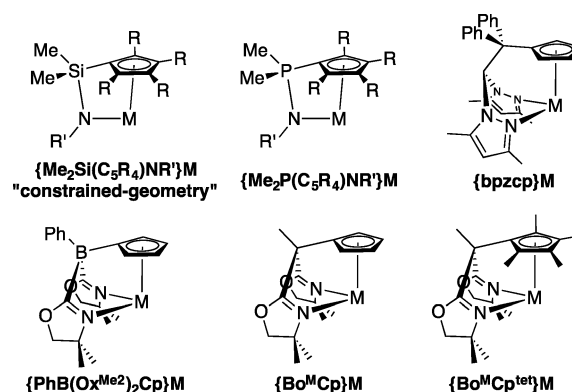


INTRODUCTION

Early metal piano-stool compounds of the type $(\eta^5\text{-C}_5\text{R}_5)\text{MX}_n$ are important for stabilizing reactive moieties such as alkylidenes and dinitrogen compounds,¹ and this class of compounds also provide catalytic sites for olefin polymerization.² The constrained-geometry class of catalysts $\{\text{Me}_2\text{Si}(\text{C}_5\text{R}_4)\text{NR}'\}\text{MX}$ exemplify the applications of piano-stool compounds in catalysis (Chart 1). These compounds suggest that strained systems can have further enhanced catalytic properties.³ Recently we showed that oxazolinyborate-substituted cyclopentadienyl ligands provide highly active and enantioselective piano-stool zirconium and hafnium hydroamination/cyclization catalysts.⁴ This reactivity contrasts with that reported for constrained-geometry group 4 catalysts in hydroamination, which require more forcing conditions.⁵

Trivalent rare earth catalysts supported by constrained-geometry-type ligands are highly reactive for hydroamination/cyclization reactions,⁶ in contrast to the group 4 examples. Monoanionic constrained-geometry-like cyclopentadienyl phosphazene or 2,2-bis(pyrazol-1-yl)ethyl lutetium dialkyl compounds ($\text{bpzcp}\}\text{Lu}(\text{CH}_2\text{SiMe}_3)_2$ ($\text{bpzcp} = 2\text{-}[2,2\text{-bis}(3,5\text{-dimethylpyrazol-1-yl})\text{-1,1-diphenylethyl}]\text{-1,3-cyclopentadiene}$) also catalyze the cyclization of aminoalkenes to 2-alkylpyrrolidines.⁷ However, group 4 piano-stool-type compounds

Chart 1. Linked Cyclopentadienyl–Donor Ligand Complexes Providing Piano-Stool Geometry Compounds



supported by monoanionic cyclopentadienyl ligands have not been explored in catalytic hydroamination.

The closest examples are dianionic ligands noted above, namely, the constrained-geometry class and our examples

Received: September 9, 2015

involving cyclopentadienyl-bis(oxazolonyl)borates.^{5,8} High oxidation state d^0 group 4 compounds are distinguished from rare earth catalysts by the valence of the metal center, with the latter class of compounds having one fewer valence, assuming the ancillary ligands' valence are equivalent. Thus, another approach to controlling the available reactive valence is through modification of the ancillary ligands' valence requirements. Given the high activity of group 4 compounds supported by these dianionic $[\text{PhB}(\text{Ox}^{\text{R}})_2\text{C}_5\text{H}_4]^{2-}$ ligands,^{4a,c,d} we targeted corresponding monoanionic $[\text{RC}(\text{Ox}^{\text{R}'})_2\text{C}_5\text{R}''_4]^-$ ligands, which might impart high reactivity upon group 4 metal sites in hydroamination and allow further comparisons in the series of compounds $\{\text{PhB}(\text{Ox}^{\text{R}})_2\text{C}_5\text{H}_4\}\text{LnX}$, $\{\text{PhB}(\text{Ox}^{\text{R}})_2\text{C}_5\text{H}_4\}\text{MX}_2$, $\{\text{RC}(\text{Ox}^{\text{R}'})_2\text{C}_5\text{R}''_4\}\text{LnX}_2$, and $\{\text{RC}(\text{Ox}^{\text{R}'})_2\text{C}_5\text{R}''_4\}\text{MX}_3$ (Ln = trivalent group 3 or lanthanide element, M = tetravalent group 4 metal center, X = monovalent ligand).

Typically, cyclopentadienyl ligand derivatives are synthesized by reaction of a nucleophilic $\text{C}_5\text{R}_4\text{H}^-$ anion and an electrophile such as a halosilane. The monoanionic cyclopentadienylphosphazene ligands are also synthesized through the reaction of $\text{C}_5\text{R}_4\text{H}^-$ and R_2PCL .⁹ Alternatively, reactions of fulvene derivatives with nucleophiles provide a CR_2 linker between the cyclopentadiene and donor groups, such as in bis-(pyrazolyl)ethylcyclopentadienyl ligands (bpzcp).¹⁰

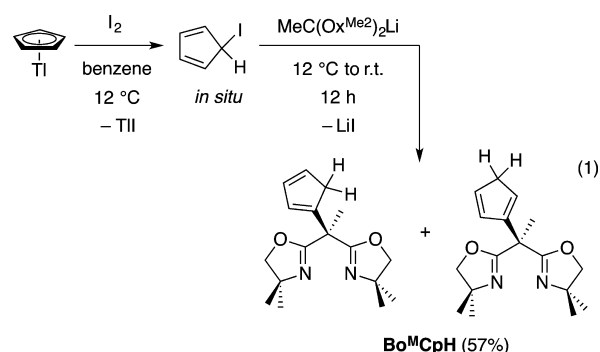
The above routes imply that preparation of one-carbon-linked analogues of $[\text{PhB}(\text{Ox}^{\text{R}})_2\text{C}_5\text{H}_4]^{2-}$ would involve coupling of two typically nucleophilic cyclopentadienide and $[\text{RC}(\text{Ox}^{\text{R}'})_2]^-$ species. Instead, we investigated a strategy for coupling the stabilized anions of bis(oxazolines) with electrophilic cyclopentadienyl groups.¹¹ The reaction of deprotonated bis(oxazoline) and organic electrophiles has been very useful to obtain tris(oxazolonyl)ethane (tris-ox) ligands¹² or side-arm-containing bis(oxazolines) that show improved enantioselectivity in a host of catalytic conversions.¹³ Recently, we reported the synthesis of the tetramethylcyclopentadienyl ligand $\text{MeC}(\text{Ox}^{\text{Me}2})_2\text{C}_5\text{Me}_4\text{H}$ ($\text{Ox}^{\text{Me}2}$ = 4,4-dimethyl-2-oxazoline) and a series of lutetium compounds coordinated by this ligand.¹⁴

Here we describe the full synthesis of achiral monoanionic cyclopentadienyl bis(oxazoline) compounds, magnesium and thallium main group compounds, and titanium and zirconium compounds. We also report an initial study of the magnesium and zirconium compounds' reactivity in hydroamination of aminoalkenes. Comparisons between the parent $\text{CpZr}(\text{NMe}_2)_3$, the new bis(oxazoline)-substituted cyclopentadienyl zirconium derivative, and previously reported bis(oxazolonyl)borate-substituted zirconium catalysts suggest trends in hydroamination activity corresponding to cyclopentadienyl substitution and the metal center's reactive valence number.

RESULTS AND DISCUSSION

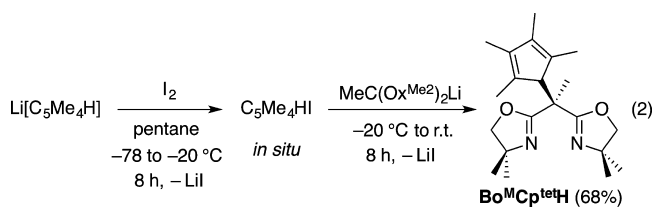
Synthesis and Characterization of Bis(4,4-dimethyl-2-oxazoline)cyclopentadiene ($\text{Bo}^{\text{M}}\text{CpH}$) and Bis(4,4-dimethyl-2-oxazoline)tetramethylcyclopentadiene ($\text{Bo}^{\text{M}}\text{Cp}^{\text{tet}}\text{H}$). The desired mixed cyclopentadiene-bis(2-oxazoline) proligands are synthesized by reaction of nucleophilic lithium bis(2-oxazolonyl)methylcarbide and iodocyclopentadiene reagents. In the first example, reaction of $\text{C}_5\text{H}_5\text{I}$ and $\text{MeC}(\text{Ox}^{\text{Me}2})_2\text{Li}$ provides $\text{MeC}(\text{Ox}^{\text{Me}2})_2\text{C}_5\text{H}_5$ ($\text{Bo}^{\text{M}}\text{CpH}$, eq 1). For this reaction, iodocyclopentadiene is generated from thallium cyclopentadienide and iodine in benzene at 12 °C and used in situ.¹¹

At least three isomers of $\text{Bo}^{\text{M}}\text{CpH}$ are possible, the structures of which are related by the position of the unique H on the



C_5H_5 group. The ^1H NMR spectrum acquired in benzene- d_6 contained two $\text{MeC}(\text{Ox}^{\text{Me}2})_2\text{C}_5\text{H}_5$ resonances at 2.10 and 2.04 ppm (normalized to 6 H total) that appeared in a 1.15:1 integrated ratio. In addition, two singlets at 3.46 and 2.73 ppm (4 H total) were assigned to sp^3 -hybridized portions of the C_5H_5 , whereas the signals assigned to sp^2 -hybridized cyclopentadienyl group integrated to a total of 6 H. From these data, two isomers are present that contain C–C connectivities with the bis(oxazoline) group bonded to an sp^2 -hybrid carbon on the C_5H_5 unit. The IR spectrum of $\text{Bo}^{\text{M}}\text{CpH}$ contained a band at 1656 cm^{-1} assigned to the oxazoline ν_{CN} , and this is the only band in this region. Interestingly, the IR spectrum of the borato compound $\text{H}[\text{PhB}(\text{Ox}^{\text{Me}2})_2\text{C}_5\text{H}_5]$, which is isolated as a mixture of three isomers and contains a H that is likely bonded to one or both oxazolines, also contained only one ν_{CN} band, but that band was red-shifted by ca. 60 cm^{-1} in comparison to $\text{Bo}^{\text{M}}\text{CpH}$.^{4a} We attribute this significant change in energy of the ν_{CN} to the substitution of a four-coordinate anionic boron in $\text{PhB}(\text{Ox}^{\text{Me}2})_2\text{Cp}$ for a neutral carbon linker in $\text{Bo}^{\text{M}}\text{Cp}$, and this may hint at inequivalent coordination properties of the oxazoline donors in the two ligands.

The generality of this synthetic approach is supported by the synthesis of the bulkier tetramethylcyclopentadienyl derivative. $\text{C}_5\text{Me}_4\text{HI}$ ¹⁵ is allowed to react with $\text{MeC}(\text{Ox}^{\text{Me}2})_2\text{Li}$ to provide $\text{MeC}(\text{Ox}^{\text{Me}2})_2\text{C}_5\text{Me}_4\text{H}$ ($\text{Bo}^{\text{M}}\text{Cp}^{\text{tet}}\text{H}$) as a white solid in 68% yield (eq 2). As noted above, we recently reported the



application of $\text{Bo}^{\text{M}}\text{Cp}^{\text{tet}}\text{H}$ in the synthesis of piano-stool lutetium compounds,¹⁴ while the synthesis and characterization of the organic compound are reported here.

In contrast to $\text{Bo}^{\text{M}}\text{CpH}$, $\text{Bo}^{\text{M}}\text{Cp}^{\text{tet}}\text{H}$ was isolated as only one isomer from this reaction, although a second isomer crystallized from a hydrolyzed organometallic compound (see below and the Supporting Information (SI)). This formulation was suggested by the diagnostic signal from $\text{MeC}(\text{Ox}^{\text{Me}2})_2\text{C}_5\text{Me}_4\text{H}$ that appeared at 1.61 and 16.41 ppm in the ^1H and $^{13}\text{C}\{^1\text{H}\}$ NMR spectra. Two singlet and two coupled doublet ^1H NMR signals were assigned to diastereotopic methyl and methylene oxazoline moieties, indicating that the oxazoline groups are equivalent. These data indicate that $\text{Bo}^{\text{M}}\text{Cp}^{\text{tet}}\text{H}$ is C_s symmetric, placing the proton on the sp^3 -hybridized C12 (identified in Figure 1). The infrared spectrum of $\text{Bo}^{\text{M}}\text{Cp}^{\text{tet}}\text{H}$ contained two

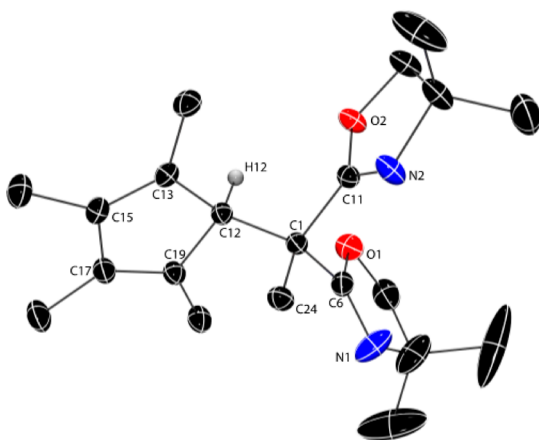


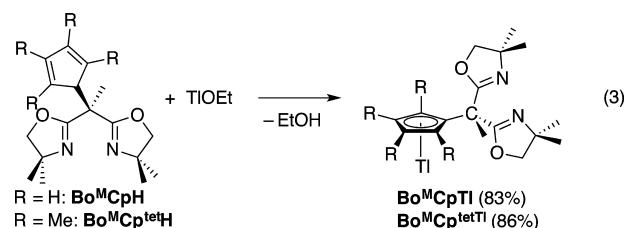
Figure 1. Rendered thermal ellipsoid diagram of MeC-(Ox^{Me2})₂C₅Me₄H (Bo^MCp^{tet}H) with ellipsoids plotted at 35% probability. H atoms were placed in calculated positions, refined isotopically using the riding model, and excluded from the illustration for clarity, with the exception of the H atom on C12. Selected interatomic distances (Å): C1–C12, 1.567(2); C1–C6, 1.521(1); C1–C11, 1.521(1); C1–C24, 1.532(2); C12–C13, 1.521(2); C12–C19, 1.521(2); C13–C15, 1.346(2); C15–C17, 1.477(2); C17–C19, 1.350(2); C6–N1, 1.247(2); C11–N2, 1.260(2). Selected interatomic angles (deg): C1–C12–C13, 112.7(1); C1–C12–C19, 114.8(1); C13–C12–C19, 103.0(1).

bands at 1661 and 1640 cm⁻¹, which were assigned to symmetric and asymmetric ν_{CN} . These two bands for a single isomer contrast the single ν_{CN} signal observed for the multiple isomers of Bo^MCpH and H[PhB(Ox^{Me2})₂C₅H₅] noted above. X-ray-quality crystals of Bo^MCp^{tet}H were obtained from a pentane solution at -30 °C (Figure 1).

The single-crystal diffraction study confirms the connectivity and the electronic configuration of the cyclopentadiene group in Bo^MCp^{tet}H. Thus, the C1 connects two oxazoline, a methyl, and a tetramethylcyclopentadienyl group. Moreover, the cyclopentadienyl C12 linked to the bis(oxazoline) unit is sp³ hybridized, determined on the basis of single bonds to neighboring carbons (~1.5 Å), the sum of C–C12–C angles of 335°, and the C–C distances in the diene portion of the C₅Me₄HR ring. Interestingly, the molecule adopts a conformation that gives a noncrystallographical pseudomirror plane, which contains the C1, C12, H12, and C24, bisects the C₅Me₄ moiety, and relates the two oxazolines. A second X-ray-quality crystal of Bo^MCp^{tet}H was obtained from the hydrolysis of a magnesium complex (see below) that proved to be an isomer in which the H atom bonded to the cyclopentadiene is located on the C13 rather than C12 (see the Supporting Information). This second isomer was not detected in the NMR spectra of characterized material.

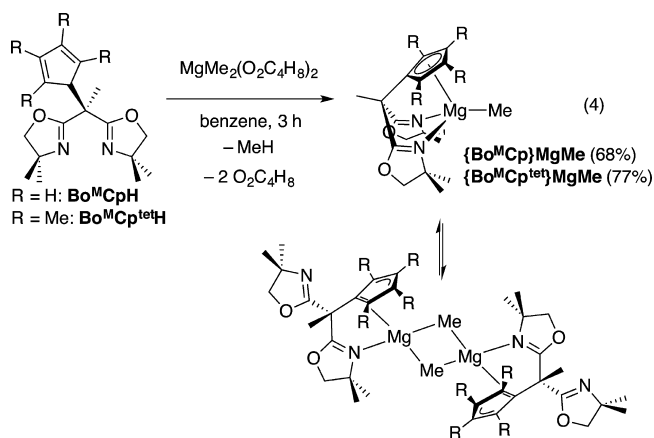
Main Group Compounds {Bo^MCp}M and {Bo^MCp^{tet}}M (M = Mg, Tl). Metalation of Bo^MCpH and Bo^MCp^{tet}H is achieved through protonolysis of Brønsted basic X-type ligands in MX_n compounds. This route provides access to thallium reagents that are useful for transmetalation. Reactions of Bo^MCpH or Bo^MCp^{tet}H and thallium ethoxide provide Bo^MCpTl or Bo^MCp^{tet}Tl (eq 3). The formation of Bo^MCpTl occurs over 2 h in diethyl ether at room temperature and is significantly faster than the synthesis of Bo^MCp^{tet}Tl, which requires 10 days in THF.

The ¹H and ¹³C{¹H} NMR spectra of Bo^MCpTl and Bo^MCp^{tet}Tl indicate that each compound is a single C₅-



symmetric isomer. The ¹H NMR spectra of Bo^MCpTl and Bo^MCp^{tet}Tl did not show evidence of coupling to the thallium (²⁰³Tl and ²⁰⁵Tl are *I* = 1/2). The cyclopentadienyl resonances in the ¹³C{¹H} NMR spectrum of Bo^MCpTl also did not contain evidence for *J*_{TlC}; however, the spectrum of Bo^MCp^{tet}Tl contained two broad signals at 114.8 ppm (38 Hz at half-height) and 114.1 ppm (and 30 Hz at half-height) and one sharper signal at 115.94 ppm (8 Hz at half-height). In addition, the C₅Me₄ methyl groups appeared as doublets at 12.6 ppm (*J*_{TlC} = 57.4 Hz) and 11.1 ppm (*J*_{TlC} = 44.8 Hz). For comparison, the methyl groups in C₅Me₅Tl provided a doublet (*J*_{TlC} = 79.4 Hz), as did the cyclopentadienyl carbons (114.6 ppm, *J*_{TlC} = 102.2 Hz).¹⁶ The ¹⁵N NMR chemical shifts, determined by ¹H–¹⁵N HMBC experiments (at ¹⁵N natural abundance) are -130 and -128 ppm, respectively, and these are in the region of noncoordinated oxazoline (e.g., 2*H*-4,4-dimethyl-2-oxazoline: -128 ppm).¹⁷ The IR spectra (acquired in a KBr matrix) of Bo^MCpTl and Bo^MCp^{tet}Tl contained one (1647 cm⁻¹) and two (1654 and 1637 cm⁻¹) bands, respectively, assigned to the ν_{CN} . Thus, both Bo^MCpH and Bo^MCpTl each produced one similar ν_{CN} IR band, while the spectra for both Bo^MCp^{tet}H and Bo^MCp^{tet}Tl contained two ν_{CN} bands. The IR bands for the Tl derivatives were slightly red-shifted in comparison to the protonated ligands.

Magnesium cyclopentadienyl compounds are also reagents for transmetalation, and oxazoline-coordinated magnesium compounds have applications as catalysts.¹⁸ The reactions of MgMe₂(O₂C₄H₈)₂ and Bo^MCpH or Bo^MCp^{tet}H give the magnesium methyl complexes {Bo^MCp}MgMe and {Bo^MCp^{tet}}MgMe (eq 4). These compounds are isolated as



off-white solids and are best stored at -30 °C to avoid thermal decomposition. In addition, we note that the carbon combustion analyses of both {Bo^MCp}MgMe and {Bo^MCp^{tet}}MgMe are consistently low, while hydrogen and nitrogen values are close to the expected values. In general, isolation of the magnesium compounds was challenging, and typically their reactivity was surveyed by in situ generated species and later repeated and verified with isolated materials.

These magnesium compounds are pseudo- C_5 symmetric at room temperature, as determined by ^1H and $^{13}\text{C}\{^1\text{H}\}$ NMR spectra acquired of benzene- d_6 solutions. However, the structures are more complicated than pentahapto cyclopentadienyl and bidentate oxazoline coordination as suggested by several pieces of data including an X-ray crystal structure of $\{\text{Bo}^{\text{M}}\text{Cp}^{\text{tet}}\}\text{MgMe}$ (see below). For example, the ^1H NMR signals of $\{\text{Bo}^{\text{M}}\text{Cp}\}\text{MgMe}$ were sharp for in situ generated samples that contained dioxane, but broad signals were obtained from samples dried by evaporation of all volatiles and redissolution in benzene- d_6 . The spectra of isolated, exhaustively dried $\{\text{Bo}^{\text{M}}\text{Cp}^{\text{tet}}\}\text{MgMe}$ were broad as well. Addition of THF to the samples that gave broad NMR signals resulted in reproducibly sharp ^1H NMR signals, equivalent to spectra obtained from in situ samples. We conclude that drying removes coordinated ethers and affects the appearance of NMR spectra, but drying does not result in demetalation or protonation of the cyclopentadienyl ligands. Moreover, the ^1H and ^{13}C NMR chemical shifts of dioxane, THF, or Et_2O in the presence of the cyclopentadienylmagnesium compounds were identical or nearly identical to the ethers' resonances in only benzene- d_6 .

The NMR data discussed here describe dioxane-containing samples (<1 equiv). Two C_5H_4 signals at 6.44 and 6.33 ppm and two C_5Me_4 methyls at 2.33 and 2.24 ppm were observed in the ^1H NMR spectra of $\{\text{Bo}^{\text{M}}\text{Cp}\}\text{MgMe}$ and $\{\text{Bo}^{\text{M}}\text{Cp}^{\text{tet}}\}\text{MgMe}$, respectively, as were the typical two oxazoline methyl signals and two coupled diastereotopic CH_2 resonances associated with C_s structures. The magnesium methyl resonances appeared as broad singlets at -0.05 and -0.9 in the ^1H NMR spectra of $\{\text{Bo}^{\text{M}}\text{Cp}\}\text{MgMe}$ and $\{\text{Bo}^{\text{M}}\text{Cp}^{\text{tet}}\}\text{MgMe}$, respectively. At the same time, the cyclopentadienyl-bis(oxazoline) signals were sharp, further indicating complex structures. Moreover, the ^1H NMR spectrum of $\{\text{Bo}^{\text{M}}\text{Cp}^{\text{tet}}\}\text{MgMe}$ acquired at -63 °C contained four methyl resonances and four coupled diastereotopic CH_2 resonances assigned to inequivalent oxazoline groups, and four signals were observed for cyclopentadienyl methyl groups. Thus, the low-temperature structure is C_1 symmetric. The magnesium methyl and 2-C of the oxazoline were difficult to observe in the $^{13}\text{C}\{^1\text{H}\}$ NMR spectra of these compounds, either generated in situ or of isolated materials. However, with small amounts of dioxane, the MgMe resonance was observed at -11 ppm. Interestingly, ^{15}N NMR signals were observed as weak cross-peaks at -146 ppm for $\{\text{Bo}^{\text{M}}\text{Cp}^{\text{tet}}\}\text{MgMe}$ and -147 ppm for $\{\text{Bo}^{\text{M}}\text{Cp}\}\text{MgMe}$ using $^1\text{H}-^{15}\text{N}$ HMBC experiments (room temperature), and these chemical shifts are ca. 20 ppm upfield of 4,4-dimethyl-2-oxazoline (-128 ppm) referenced in the above discussion.

In addition, the infrared spectra (in KBr) of powdered samples of $\{\text{Bo}^{\text{M}}\text{Cp}\}\text{MgMe}$ and $\{\text{Bo}^{\text{M}}\text{Cp}^{\text{tet}}\}\text{MgMe}$, obtained by evaporation of frozen benzene solutions, each contained a single band in the region associated with the $\text{C}=\text{N}$ stretch of the oxazoline group at 1658 cm^{-1} . The observation of one IR band contrasts the spectra of $\text{Bo}^{\text{M}}\text{Cp}^{\text{tet}}\text{H}$ and $\text{Bo}^{\text{M}}\text{Cp}^{\text{tet}}\text{I}$, which contained two ν_{CN} bands. One IR band is commonly observed in tridentate tris(oxazolanyl)borate compounds, and we attribute this to weak intensity of the asymmetric mode. For example, $\text{To}^{\text{M}}\text{MgMe}$ ($\text{To}^{\text{M}} = \text{tris}(4,4\text{-dimethyl-2-oxazolanyl})\text{-phenylborate}$) is C_{3v} symmetric, all three oxazolines are coordinated to magnesium(II), its ^{15}N NMR chemical shift is -157 ppm, and the ν_{CN} absorption appears at 1592 cm^{-1} in the

IR spectrum.^{18a} A similar effect may account for the single ν_{CN} in $\{\text{Bo}^{\text{M}}\text{Cp}\}\text{MgMe}$ and $\{\text{Bo}^{\text{M}}\text{Cp}^{\text{tet}}\}\text{MgMe}$.

Support for a dimeric structure is obtained in the solid state from an X-ray diffraction study on $\{\text{Bo}^{\text{M}}\text{Cp}^{\text{tet}}\}\text{MgMe}$. The results indicate that only one oxazoline ring coordinates per magnesium, and the methyl groups bridge between the two magnesium centers (Figure 2). The cyclopentadienyl group

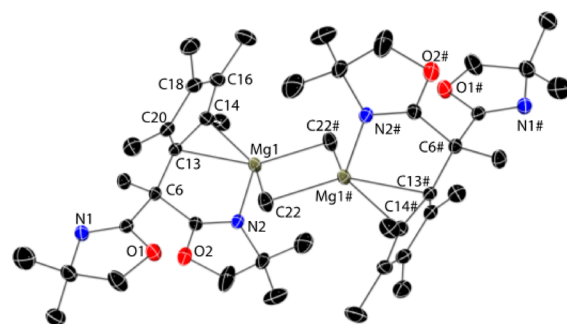


Figure 2. Rendered thermal ellipsoid plot of $[\{\text{Bo}^{\text{M}}\text{Cp}^{\text{tet}}\}\text{MgMe}]_2$ at 35% probability. H atoms are not included in the representation. Atoms marked with # are crystallographic symmetry-generated positions. Selected interatomic distances (Å): Mg1–C22, 2.267(2); Mg1–C22#, 2.271(2); Mg1–N2, 2.214(1); Mg1–C13, 2.284(2); Mg1–C14, 2.400(2); Mg1–C16, 2.681(2); Mg1–C18, 2.821(2); Mg1–C20, 2.658(2); C13–C14, 1.437(2); C14–C16, 1.412(2); C16–C18, 1.404(2); C18–C20, 1.410(2), C13–C20, 1.421(2).

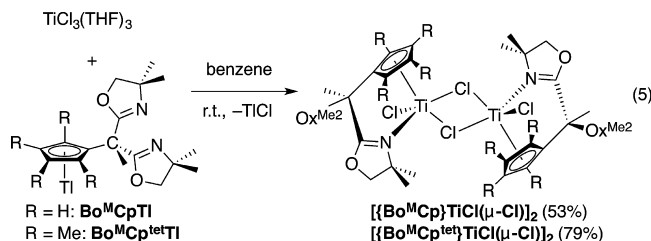
coordinates to the magnesium center through a $\eta^2\text{-C}_5\text{Me}_4\text{R}$ interaction in which the magnesium–carbon distances are inequivalent. The short Mg–C distances involve the bis(oxazoline)-substituted carbon (Mg1–C13, 2.384(2) Å) and the adjacent carbon (Mg1–C14, 2.400(2) Å). The next shorter distances of Mg1–C16 and Mg1–C20, 2.681(2) and 2.658(2) Å, respectively, are significantly longer. The magnesium–carbon distances of the bridging methyl groups are similar but unequal (Mg1–C22, 2.267(2) and Mg1–C22#, 2.271(2) Å) and similar to the shortest distance in the magnesium–cyclopentadienyl interaction. The bridging Mg–C distances are similar to those in $[(\text{C}_5\text{Me}_4\text{Et})\text{Mg}(\mu\text{-Me})\text{THF}]_2$.¹⁹ This structure is distinguished from the monomeric structures obtained with $\kappa^2\text{-}\eta^5\text{-}\{\text{HC}(\text{Pz}^{\text{Me}_2})_2(\text{Ph}_2\text{CC}_5\text{H}_4)\}\text{MgR}$ ($\text{Pz}^{\text{Me}_2} = 3,5\text{-dimethylpyrazolyl}$; $\text{R} = \text{CH}_2\text{SiMe}_3$, ^tBu),²⁰ although a number of cyclopentadienyl magnesium piano-stool compounds have been crystallographically characterized to contain monohapto to pentahapto coordination modes, including $(\eta^1\text{-C}_5\text{H}_5)(\eta^5\text{-C}_5\text{H}_5)\text{MgTHF}_2$.²¹

Notably, the solid-state IR spectrum of amorphous material suggests equivalent oxazolines. Therefore, crystallized $\{\text{Bo}^{\text{M}}\text{Cp}^{\text{tet}}\}\text{MgMe}$ was subjected to IR analysis, which revealed two ν_{CN} peaks at 1657 and 1628 cm^{-1} . The two bands in this spectrum are consistent with expectations based on the X-ray diffraction study, with the lower energy band assigned to the coordinated oxazoline.

The solution-phase structure might involve formation of a dimeric species, so the diffusion rate was measured by ^1H DOSY experiments and compared to known monomeric magnesium species. The diffusion constant for $\{\text{Bo}^{\text{M}}\text{Cp}^{\text{tet}}\}\text{MgMe}$ (392.25 amu as a monomer) is $7.9 \times 10^{-10}\text{ m}^2/\text{s}$ (at 23.5 mM), whereas the diffusion constants of monomeric $\text{To}^{\text{M}}\text{MgSi}(\text{SiHMe}_2)_3$ (611.29 amu) and $\text{To}^{\text{M}}\text{MgMe}$ (421.24 amu) are 6.95×10^{-10} and $8.5 \times 10^{-10}\text{ m}^2/\text{s}$,²² respectively. The value of $\{\text{Bo}^{\text{M}}\text{Cp}^{\text{tet}}\}\text{MgMe}$ is between these two

compounds, suggesting an averaged molecular weight of rapidly exchanging monomer and dimers.

Group 4 $\{\text{Bo}^{\text{M}}\text{Cp}\}\text{M}$ and $\{\text{Bo}^{\text{M}}\text{Cp}^{\text{tet}}\}\text{M}$ ($\text{M} = \text{Ti}, \text{Zr}$) Compounds. The reactions of $\text{TiCl}_3(\text{THF})_3$ with $\text{Bo}^{\text{M}}\text{CpTi}$ or $\text{Bo}^{\text{M}}\text{Cp}^{\text{tet}}\text{Ti}$ provide paramagnetic $[\{\text{Bo}^{\text{M}}\text{Cp}\}\text{TiCl}(\mu\text{-Cl})]_2$ or $[\{\text{Bo}^{\text{M}}\text{Cp}^{\text{tet}}\}\text{TiCl}(\mu\text{-Cl})]_2$ (eq 5).



The infrared spectrum of $[\{\text{Bo}^{\text{M}}\text{Cp}\}\text{TiCl}(\mu\text{-Cl})]_2$ acquired in a KBr matrix contained two signals at 1662 and 1635 cm^{-1} , which were assigned to CN stretching modes of non-coordinated and coordinated oxazoline groups. Similarly, the infrared spectrum of $[\{\text{Bo}^{\text{M}}\text{Cp}^{\text{tet}}\}\text{TiCl}(\mu\text{-Cl})]_2$ contained ν_{CN} bands at 1661 and 1641 cm^{-1} . The structures of these two compounds were assigned based on the correspondence of the IR data to the dimeric structure of $[\{\text{Bo}^{\text{M}}\text{Cp}\}\text{TiCl}(\mu\text{-Cl})]_2$ indicated by a single-crystal X-ray diffraction study (see below) and EPR data.

Although the ^1H NMR signals appeared in the typical region at 0–7 ppm, the spectra of $[\{\text{Bo}^{\text{M}}\text{Cp}\}\text{TiCl}(\mu\text{-Cl})]_2$ or $[\{\text{Bo}^{\text{M}}\text{Cp}^{\text{tet}}\}\text{TiCl}(\mu\text{-Cl})]_2$ were not initially useful for assigning structure or monitoring reaction progress because of the d^1 Ti(III) centers. The ^1H NMR spectrum of $[\{\text{Bo}^{\text{M}}\text{Cp}\}\text{TiCl}(\mu\text{-Cl})]_2$ contained three broad aliphatic resonances at 0.5, 0.8, and 1 ppm likely from methyl groups present in the $\text{Bo}^{\text{M}}\text{Cp}$ ligand, and these were the most intense signals in the spectrum. Cyclopentadienyl signals were barely detected. In the ^1H NMR spectrum of $[\{\text{Bo}^{\text{M}}\text{Cp}^{\text{tet}}\}\text{TiCl}(\mu\text{-Cl})]_2$, ca. 20 signals at 0.5–2.0 ppm were observed. Despite the complex spectrum, multiple preparations provided reproducible ^1H NMR spectra with these signals assigned to methyl groups in C_5Me_4 and Ox^{Me_2} moieties. All these signals were weak with respect to the residual benzene- d_6 signal, but unlike monomeric Cp^*TiCl , these methyl signals are not paramagnetically shifted.²³ In addition, we note that carbon combustion analyses were consistently lower than expected, although hydrogen and nitrogen match calculated values.

The room-temperature magnetic susceptibility values (measured by Evan's method) were 1.60 μ_{B} (0.886 e^-) and 1.25 μ_{B} (0.69 e^-) per Ti center. Electron paramagnetic resonance (EPR) experiments on point samples measured at room temperature provided g -values of 1.984 and 1.989 for $[\{\text{Bo}^{\text{M}}\text{Cp}\}\text{TiCl}(\mu\text{-Cl})]_2$ and $[\{\text{Bo}^{\text{M}}\text{Cp}^{\text{tet}}\}\text{TiCl}(\mu\text{-Cl})]_2$, respectively. Moreover, EPR spectra of glassed 9 mM toluene solutions of $[\{\text{Bo}^{\text{M}}\text{Cp}\}\text{TiCl}(\mu\text{-Cl})]_2$ and $[\{\text{Bo}^{\text{M}}\text{Cp}^{\text{tet}}\}\text{TiCl}(\mu\text{-Cl})]_2$ measured at 10 K contained a signal at half-field that indicated the presence of a triplet diradical in the samples. The triplet signal is also observed for $(\text{Cp}_2\text{TiCl})_2$,²⁴ and that compound also exhibits weak antiferromagnetic coupling of the two d^1 Ti(III) centers.²⁵ Thus, the EPR spectrum provides additional evidence for dimeric structures of the two titanium(III) compounds. In contrast, the triplet EPR signal was not observed in glassed 2-methyl THF at 10 K.

X-ray-quality crystals of $[\{\text{Bo}^{\text{M}}\text{Cp}\}\text{TiCl}(\mu\text{-Cl})]_2$ were obtained from a toluene/pentane solution cooled at -30 °C

(Figure 3). The compound crystallizes as a dimer with each Ti coordinated in a four-legged piano-stool geometry, with two

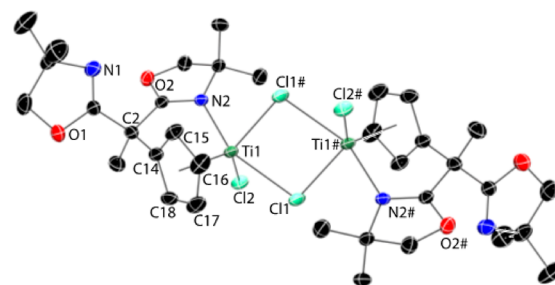
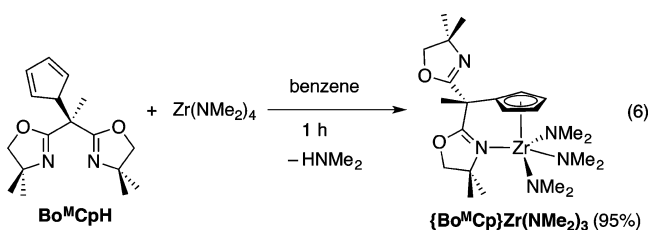


Figure 3. Rendered thermal ellipsoid plot of $[\{\text{Bo}^{\text{M}}\text{Cp}\}\text{TiCl}(\mu\text{-Cl})]_2$. Ellipsoids are plotted at 35% probability, and H atoms are not illustrated for clarity. Selected interatomic distances (Å): Ti1–Cl1, 2.435(1); Ti1–Cl1#, 2.570(1); Ti1–Cl2, 2.366(1); Ti1–N2, 2.238(2); Ti1–C14, 2.328(3); Ti1–C15, 2.312(4); Ti1–C16, 2.339(4); Ti1–C17, 2.396(4); Ti1–C18, 2.404(4); Ti1–Ti1#, 3.844(2); C14–C15, 1.429(5); C15–C16, 1.415(4); C16–C17, 1.424(6); C17–C18, 1.393(6); C18–C14, 1.418(4).

bridging chloride ligands, a terminal chloride, the cyclopentadienyl group, and one oxazoline ligand. The two $\{\text{Bo}^{\text{M}}\text{Cp}\}\text{Ti}$ groups in the dimer are related by a crystallographically imposed inversion center. The Ti–Ti distance is 3.844(2) Å, which is slightly smaller than the distances of 3.943(2) and 3.926(3) Å in $[\text{Cp}_2\text{Ti}(\mu\text{-Cl})]_2$ and $[(\text{C}_5\text{H}_4\text{Me})_2\text{Ti}(\mu\text{-Cl})]_2$.²⁵ Only one oxazoline ring coordinates per titanium center, and a similar pentahapto-monodentate coordination is observed for the zirconium compound $\{\text{Bo}^{\text{M}}\text{Cp}\}\text{Zr}(\text{NMe}_2)_3$ described below.

The terminal Ti1–Cl2 is the shortest distance (2.366(1) Å) of the three Ti–Cl bonds, and the two bridging Ti1–Cl1–Ti1# interactions have inequivalent Ti–Cl distances (Ti1–Cl1, 2.435(1); Ti1–Cl1#, 2.570(1) Å). The unequal bridging Ti–Cl distances also contrast the molecular structures of $[\text{Cp}_2\text{Ti}(\mu\text{-Cl})]_2$ and $[(\text{C}_5\text{H}_4\text{Me})_2\text{Ti}(\mu\text{-Cl})]_2$, which contain similar internal distances (e.g., in the latter, Ti–Cl = 2.566(2), 2.526(2), 2.535(2), and 2.562(2) Å).

The reaction of $\text{Bo}^{\text{M}}\text{CpH}$ and $\text{Zr}(\text{NMe}_2)_4$ in benzene at room temperature yields $\{\text{Bo}^{\text{M}}\text{Cp}\}\text{Zr}(\text{NMe}_2)_3$ with the loss of dimethylamine (eq 6). However, $\text{Bo}^{\text{M}}\text{Cp}^{\text{tet}}\text{H}$ does not react with $\text{Zr}(\text{NMe}_2)_4$ in benzene or THF, even at elevated temperatures up to 120 °C over 2 days.



A ^1H NMR spectrum of a micromolar-scale reaction showed that $\{\text{Bo}^{\text{M}}\text{Cp}\}\text{Zr}(\text{NMe}_2)_3$ forms within 10 min at room temperature. A singlet resonance at 3.08 ppm (18 H) in the ^1H NMR spectrum was assigned to the apparently equivalent NMe_2 groups. In addition, one set of oxazoline signals, with two signals corresponding to inequivalent methyl and two doublets assigned to diastereotopic methylenes, was observed in the spectrum acquired at room temperature. At -70 °C, the oxazolines were inequivalent and revealed four methyl

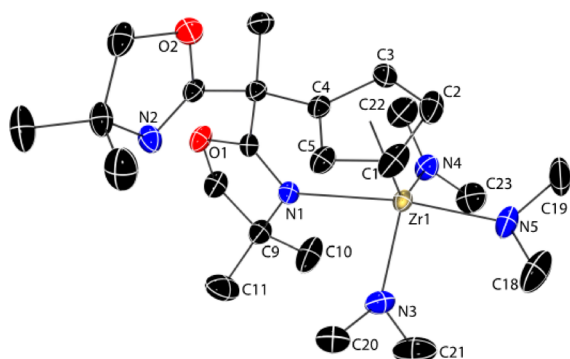


Figure 4. Rendered thermal ellipsoid plot of $\text{Bo}^{\text{M}}\text{CpZr}(\text{NMe}_2)_3$. H atoms are not depicted for clarity. Selected interatomic distances (Å): Zr1–C1, 2.573(2); Zr1–C2, 2.580(2); Zr1–C3, 2.617(2); Zr1–C4, 2.641(2); Zr1–C5, 2.599(2); Zr1–N1, 2.536(1); Zr1–N3, 2.071(2); Zr1–N4, 2.092(1); Zr1–N5, 2.101(2). Selected angles (deg): N1–Zr1–N5, 163.36(6), N3–Zr1–N4, 120.40(6).

resonances. Four cyclopentadienyl signals also appeared. The NMe_2 signal broadened from its sharp nature at room temperature to a broad signal that overlapped with oxazoline methylene signals at -78°C . Thus, at room temperature, the

coordinated and noncoordinated oxazolines exchange rapidly. The exchange process is slowed at low temperature, while a second process that affects the NMe_2 on the order of the ^1H NMR time scale occurs at -78°C .

As in the magnesium compounds described above, the ν_{CN} features in the infrared spectra varied between solution phase, amorphous material obtained from fast evaporation of solvent, and crystalline material. In benzene solution, two bands at 1659 and 1641 cm^{-1} were observed, while amorphous material (in a KBr matrix) provided a spectrum with only one ν_{CN} at 1646 cm^{-1} . $\{\text{Bo}^{\text{M}}\text{Cp}\}\text{Zr}(\text{NMe}_2)_3$ that was crystallized from a mixture of pentane and toluene provided an IR spectrum that contained two bands at 1657 and 1636 cm^{-1} . In spectra from the crystal or solution-phase samples, the low-energy band was assigned to coordinated oxazoline, and the high-energy stretch was assigned to a noncoordinated group. Presumably, both oxazolines are coordinated in the amorphous material.

A single-crystal X-ray diffraction study of $\{\text{Bo}^{\text{M}}\text{Cp}\}\text{Zr}(\text{NMe}_2)_3$ showed one coordinated and one noncoordinated oxazoline. The zirconium center adopts a four-legged piano-stool geometry, an open site *trans* to the cyclopentadienyl group. The Zr1–N1 distance of $2.536(1)\text{ Å}$ is significantly

Table 1. Catalytic Hydroamination of Aminoalkenes

| Substrate | Catalyst (10 mol%) | Temp. ($^\circ\text{C}$) | Time (h) | Conversion (%) | N_t | Yield (%) ^c | |
|--|--|--|----------|----------------|-------------|------------------------|-----------------|
| | $\{\text{Bo}^{\text{M}}\text{Cp}\}\text{MgMe}$ | 25 | 0.75 | >99 | 13 | 95 | |
| | $\{\text{Bo}^{\text{M}}\text{Cp}^{\text{tet}}\}\text{MgMe}$ | 25 | 1.5 | >99 | 6.7 | 96 | |
| | $\text{To}^{\text{M}}\text{MgMe}^{\text{d}}$ | 50 | 12 | 99 | 0.83 | 99 ^d | |
| | $\{\text{Bo}^{\text{M}}\text{Cp}\}\text{Zr}(\text{NMe}_2)_3$ | 25 | 36 | >99 | 0.28 | 86 | |
| | $\text{CpZr}(\text{NMe}_2)_3$ | 25 | 36 | 20 | 0.05 | n.a. | |
| | $\text{CpZr}(\text{NMe}_2)_3$ | 60 | 20 | >99 | 0.5 | 80 | |
| | $\{\text{Bo}^{\text{M}}\text{Cp}\}\text{Zr}(\text{NMe}_2)_3$ | 60 | 2.5 | >99 | 4 | 86 | |
| | $\{\text{PhB}(\text{O}^{\text{xMe}_2})_2\text{Cp}\}\text{Zr}(\text{NMe}_2)_2^{\text{b}}$ | 23 | 11 | 90 | 0.8 | 84 | |
| | | $\{\text{Bo}^{\text{M}}\text{Cp}\}\text{MgMe}$ | 25 | 2 | >99 (1:1.1) | 5 | 95 |
| | | $\{\text{Bo}^{\text{M}}\text{Cp}^{\text{tet}}\}\text{MgMe}$ | 25 | 2 | >99 (1:1.1) | 5 | 94 |
| | | $\{\text{Bo}^{\text{M}}\text{Cp}\}\text{Zr}(\text{NMe}_2)_3$ | 25 | 42 | >99 (1:2.8) | 0.2 | 88 |
| | | $\text{CpZr}(\text{NMe}_2)_3$ | 25 | 42 | 20 | 0.05 | n.a. |
| $\text{CpZr}(\text{NMe}_2)_3$ | | 60 | 24 | >99 (1:3) | 0.4 | 82 | |
| $\{\text{Bo}^{\text{M}}\text{Cp}\}\text{Zr}(\text{NMe}_2)_3$ | | 60 | 3 | >99 | 3.3 | 88 | |
| | $\{\text{Bo}^{\text{M}}\text{Cp}\}\text{MgMe}$ | 25 | 2 | >99 | 5 | 94 | |
| | $\{\text{Bo}^{\text{M}}\text{Cp}^{\text{tet}}\}\text{MgMe}$ | 25 | 1.5 | >99 | 6.7 | 94 | |
| | $\text{To}^{\text{M}}\text{MgMe}^{\text{d}}$ | 50 | 15 | >99 | 0.67 | 99 ^d | |
| | $\{\text{Bo}^{\text{M}}\text{Cp}\}\text{Zr}(\text{NMe}_2)_3$ | 25 | 36 | >99 | 0.28 | 88 | |
| | $\{\text{PhB}(\text{O}^{\text{xMe}_2})_2\text{Cp}\}\text{Zr}(\text{NMe}_2)_2^{\text{b}}$ | 23 | 11 | 92 | 0.84 | 87 | |
| | | $\{\text{Bo}^{\text{M}}\text{Cp}\}\text{MgMe}$ | 25 | 12 | 12 | 0.1 | 10 ^d |
| $\{\text{Bo}^{\text{M}}\text{Cp}^{\text{tet}}\}\text{MgMe}$ | | 80 | 1.5 | 50 | 3.3 | 46 ^d | |
| $\text{To}^{\text{M}}\text{MgMe}^{\text{d}}$ | | 50 | 72 | 20 | 0.03 | 20 ^d | |
| $\{\text{Bo}^{\text{M}}\text{Cp}\}\text{Zr}(\text{NMe}_2)_3$ | | 60 | 12 | 50 | 0.4 | 41 ^d | |
| $\{\text{PhB}(\text{O}^{\text{xMe}_2})_2\text{Cp}\}\text{Zr}(\text{NMe}_2)_2^{\text{b}}$ | | 23 | 11 | 85 | 0.8 | 85 | |
| | | $\{\text{Bo}^{\text{M}}\text{Cp}\}\text{MgMe}$ | 25 | 2 | >99 | 5 | 95 |
| | $\{\text{Bo}^{\text{M}}\text{Cp}^{\text{tet}}\}\text{MgMe}$ | 25 | 2 | >99 | 5 | 97 | |
| | $\{\text{Bo}^{\text{M}}\text{Cp}\}\text{Zr}(\text{NMe}_2)_3$ | 25 | 36 | >99 | 0.3 | 87 | |
| | $\{\text{PhB}(\text{O}^{\text{xMe}_2})_2\text{Cp}\}\text{Zr}(\text{NMe}_2)_2^{\text{b}}$ | 23 | 11 | 87 | 0.8 | 80 | |

^aSee ref 18a. ^bSee ref 4a. ^cIsolated yield. ^dNMR yield.

longer than the distances to the amides (Zr1–N3, 2.071(2); Zr1–N4, 2.092(1); Zr1–N5, 2.101(2) Å).

The mutually *trans* dimethylamide ligands of N3 and N4 are planar (Σ angles around N3 and N4 is 360°), while the dimethylamide of N5 (pseudo *trans* to the oxazoline) is slightly pyramidalized (Σ angles around N5 is 356°). In addition, the N5 dimethylamide is oriented with both methyls equidistant from the Cp centroid, whereas N3 and N4 dimethylamide planes are roughly orthogonal to the cyclopentadienyl plane.

Catalytic Hydroamination/Cyclization of Aminoalkenes. Catalytic cyclization reactions of aminoalkenes provide an initial test of the reactivity of the magnesium and group 4 compounds supported by these cyclopentadienyl-bis(oxazoline) ligands. These reactions also provide means for comparing reactivity with previously reported $\text{To}^{\text{M}}\text{MgMe}$,^{18a} $\text{To}^{\text{M}}\text{Zr}(\text{NMe}_2)_3$,²⁶ and $\{\text{PhB}(\text{Ox}^{\text{Me}_2})_2\text{Cp}\}\text{Zr}(\text{NMe}_2)_2$,^{4a} as well as the unsubstituted piano-stool compound $\text{CpZr}(\text{NMe}_2)_3$. It is worth noting that the amide groups in $\text{To}^{\text{M}}\text{Zr}(\text{NMe}_2)_3$ are not readily substituted and that the compound is not a good catalyst for cyclization of aminoalkenes.²⁶ $\text{CpZr}(\text{NMe}_2)_3$ is isoelectronic with $\text{To}^{\text{M}}\text{Zr}(\text{NMe}_2)_3$, but to our knowledge, the former compounds' reactivity in catalytic hydroamination/cyclization has not previously been described.

$\{\text{Bo}^{\text{M}}\text{Cp}\}\text{MgMe}$, $\{\text{Bo}^{\text{M}}\text{Cp}^{\text{tet}}\}\text{MgMe}$, and $\{\text{Bo}^{\text{M}}\text{Cp}\}\text{Zr}(\text{NMe}_2)_3$ are precatalysts for the cyclization of aminoalkenes to heterocyclic amines as reported in Table 1. Upon addition of primary amines to the magnesium methyl or zirconium dimethylamide compounds, methane or dimethylamine is observed, indicating that a metal amide is formed. Comparison of Mg and Zr catalysts with the same ancillary ligand shows that magnesium catalysts are generally more reactive than zirconium, i.e., $\text{To}^{\text{M}}\text{MgMe} > \text{To}^{\text{M}}\text{Zr}(\text{NMe}_2)_3$ and $\{\text{Bo}^{\text{M}}\text{Cp}\}\text{MgMe} > \{\text{Bo}^{\text{M}}\text{Cp}\}\text{Zr}(\text{NMe}_2)_3$. In the magnesium series, relative reaction rates show $\{\text{Bo}^{\text{M}}\text{Cp}\}\text{MgMe} \sim \{\text{Bo}^{\text{M}}\text{Cp}^{\text{tet}}\}\text{MgMe} > \text{To}^{\text{M}}\text{MgMe}$ as catalysts for aminoalkene cyclization. Notably, both $\{\text{Bo}^{\text{M}}\text{Cp}\}\text{MgMe}$ and $\{\text{Bo}^{\text{M}}\text{Cp}^{\text{tet}}\}\text{MgMe}$ readily afford pyrrolidine at room temperature. The diastereoselectivity for cyclization of amino dialkene by $\{\text{Bo}^{\text{M}}\text{Cp}\}\text{MgMe}$ or $\{\text{Bo}^{\text{M}}\text{Cp}^{\text{tet}}\}\text{MgMe}$ is 1:1.

In the zirconium series, the relative reactivity follows the trend $\{\text{PhB}(\text{Ox}^{\text{Me}_2})_2\text{Cp}\}\text{Zr}(\text{NMe}_2)_2 > \{\text{Bo}^{\text{M}}\text{Cp}\}\text{Zr}(\text{NMe}_2)_3 > \text{CpZr}(\text{NMe}_2)_3 \gg \text{To}^{\text{M}}\text{Zr}(\text{NMe}_2)_3$. At room temperature under equivalent conditions, the turnover rate for cyclization to 2-methyl-4,4-diphenylpyrrolidine by $\{\text{Bo}^{\text{M}}\text{Cp}\}\text{Zr}(\text{NMe}_2)_3$ is approximately 5× faster than $\text{CpZr}(\text{NMe}_2)_3$ but 3× slower than $\{\text{PhB}(\text{Ox}^{\text{Me}_2})_2\text{Cp}\}\text{Zr}(\text{NMe}_2)_2$. Although $\text{CpZr}(\text{NMe}_2)_3$ is the least reactive of the cyclopentadienyl-coordinated precatalysts, catalytic conversion is observed at room temperature. This activity is perhaps surprising given the few examples of zirconium complexes that catalyze hydroamination/cyclization at room temperature. For example, the N_t for constrained-geometry $\{\text{Me}_2\text{Si}(\text{C}_3\text{R}_4)\text{NR}'\}\text{ZrMe}_2$ is 0.07 h^{-1} at 100 °C in a conversion that gives 4,4-dimethyl-2-methylpyrrolidine, whereas the N_t for $\{\text{Bo}^{\text{M}}\text{Cp}\}\text{Zr}(\text{NMe}_2)_3$ is 0.4 h^{-1} at 60 °C. Interestingly, a slightly faster conversion is catalyzed by $\{\text{Me}_2\text{Si}(\text{C}_3\text{R}_4)\text{NR}'\}\text{ZrCl}(\text{NMe}_2)$ with an N_t of 0.14 h^{-1} at 100 °C.⁵ As noted above, $\text{To}^{\text{M}}\text{Zr}(\text{NMe}_2)_3$, which is isoelectronic with $\text{CpZr}(\text{NMe}_2)_3$, is not a catalyst for cyclization of aminoalkenes, and this inactivity may relate to its six-coordinate zirconium center and substitutionally inert coordination sphere.

CONCLUSIONS

These new monoanionic cyclopentadienyl-bis(oxazoline) ligands provide chelating piano-stool compounds of Ti, Mg, Ti, and Zr. The syntheses of the ligands described here employ the combination of electrophilic cyclopentadienyl derivatives with nucleophilic, stabilized bis(oxazoline) carbanions. This cyclopentadienyl ligand construction is opposite the synthesis of ansa-type dimethylsilyl-bis(cyclopentadiene) or constrained-geometry-type dimethylsilyl-cyclopentadiene-amido ligands that employ nucleophilic cyclopentadienide derivatives combined with electrophilic silicon centers.^{3b} Likewise, the synthesis of the optically active dianionic cyclopentadienyl-bis(oxazolonyl)borate ligands $[\text{PhB}(\text{Ox}^{\text{R}})_2\text{C}_5\text{H}_4]^{2-}$ involves the reaction of cyclopentadienide nucleophile NaC_5H_5 and electrophilic borane $\text{PhB}(\text{Ox}^{\text{R}})_2$.^{4a–c} Here, we have shown that reversing the electrophilic and nucleophilic components in this alternative synthetic approach has some generality in terms of varying steric properties on the cyclopentadienyl group. The synthetic approach, then, lends itself to a range of combinations through the variation of groups on the cyclopentadienyl ring as well as the substituents on the oxazoline ring. Because oxazolines are readily prepared in enantiopure chiral form with a number of substituents in the 4 and 5 positions, optically active piano-stool compounds may readily be prepared for application in asymmetric catalysis, including hydroamination. We are currently synthesizing a range of derivatives of this ligand class. Moreover, this approach may be generally useful for the synthesis of cyclopentadienyl ligands with new substitution patterns and substituents derived from nucleophiles rather than electrophiles.

In this context, it is interesting to note that the combination of the bis(oxazoline) and cyclopentadienyl ligands on zirconium gives more reactive catalytic species than the oxazoline-free $\text{CpZr}(\text{NMe}_2)_3$ catalyst precursor. We are not aware of prior studies of the parent piano-stool compound $\text{CpZr}(\text{NMe}_2)_3$ as a catalyst for cyclization of aminoalkenes, and this compound is surprisingly reactive under catalytic conditions. In contrast, the compound $\text{To}^{\text{M}}\text{Zr}(\text{NMe}_2)_3$,²⁶ which is isoelectronic with $\text{CpZr}(\text{NMe}_2)_3$, is inert toward substitution of dimethylamide groups by amines and is not an active catalyst for hydroamination/cyclization. That is, the introduction of oxazoline donors does not inherently enhance the reactivity of dimethylamido zirconium sites in hydroamination. However, the combination of cyclopentadienyl and oxazoline ligands on zirconium leads to more reactive catalytic sites than parent cyclopentadienyl or tris(oxazolonyl)borate ligands. Moreover, the comparison of zwitterionic borate complex $\{\text{PhB}(\text{Ox}^{\text{Me}_2})_2\text{Cp}\}\text{Zr}(\text{NMe}_2)_2$ with $\{\text{Bo}^{\text{M}}\text{Cp}\}\text{Zr}(\text{NMe}_2)_3$ reveals that the divalent ancillary ligand gives more reactive zirconium sites. We are continuing to study and compare these ligand classes in catalytic chemistry to further discover systematic trends of reactivity and selectivity.

EXPERIMENTAL SECTION

General Procedures. All reactions were performed under a dry argon atmosphere using standard Schlenk techniques or under a nitrogen atmosphere in a glovebox, unless otherwise indicated. Dry, oxygen-free solvents were used throughout. Benzene, toluene, pentane, methylene chloride, diethyl ether, and tetrahydrofuran were degassed by sparging with nitrogen, filtered through activated alumina columns, and stored under nitrogen. Benzene- d_6 , toluene- d_8 , and tetrahydrofuran- d_8 were heated to reflux over Na/K alloy and vacuum-transferred. Anhydrous $\text{TiCl}_3(\text{THF})_3$ and TIOEt were purchased from Aldrich and

used as received. $\text{MeHC}(\text{Ox}^{\text{Me}_2})_2$,²⁷ $\text{MgMe}_2(\text{O}_2\text{C}_4\text{H}_8)_2$,²⁸ $\text{Zr}(\text{NMe}_2)_4$,²⁹ $\text{Ti}[\text{C}_5\text{H}_5]_3$,³⁰ $\text{C}_5\text{Me}_4\text{H}_2$,³¹ $\text{Bo}^{\text{M}}\text{Cp}^{\text{tetH}}$,¹⁴ 2,2-diphenyl-4-penten-1-amine,³² 2,2-dimethyl-4-penten-1-amine,³³ (1-allylcyclohexyl)methylamine,³⁴ and C-(1-allyl-cyclopentyl)-methylamine³⁴ were prepared according to the literature. ^1H and $^{13}\text{C}\{^1\text{H}\}$ NMR spectra were collected on either a Bruker DRX-400 spectrometer, a Bruker Avance III 600 spectrometer, or an Agilent MR 400 spectrometer. ^{15}N chemical shifts were determined by ^1H - ^{15}N HMBBC experiments on a Bruker Avance III 600 spectrometer. ^{15}N chemical shifts were originally referenced to liquid NH_3 and recalculated to the CH_3NO_2 chemical shift scale by adding -381.9 ppm.

$\text{MeC}(\text{Ox}^{\text{Me}_2})_2\text{Li}$. $\text{MeHC}(\text{Ox}^{\text{Me}_2})_2$ (2.000 g, 8.92 mmol) was dissolved in pentane (50 mL), the solution was cooled to -78 °C, and $^n\text{BuLi}$ in hexane (9.0 mmol, 3.6 mL) was added. The mixture was stirred at this temperature for 2 h, and then the solution was warmed to room temperature and stirred for 12 h. The solvent was removed by filtration, and the solid product was washed with pentane (50 mL). Evaporation of residual solvent under reduced pressure provided white solid $\text{MeC}(\text{Ox}^{\text{Me}_2})_2\text{Li}$ in good yield (1.912 g, 8.3 mmol, 93%). Mp: 292–294 °C (dec). ^1H NMR (THF- d_8 , 600 MHz): δ 3.59 (s, 4 H, $\text{CNCMe}_2\text{CH}_2\text{O}$), 1.69 (s, 3 H, $\text{MeC}(\text{Ox}^{\text{Me}_2})_2$), 1.13 (s, 12 H, $\text{CNCMe}_2\text{CH}_2\text{O}$). $^{13}\text{C}\{^1\text{H}\}$ NMR (THF- d_8 , 151 MHz): δ 170.51 ($\text{CNCMe}_2\text{CH}_2\text{O}$), 77.84 ($\text{CNCMe}_2\text{CH}_2\text{O}$), 65.39 ($\text{CNCMe}_2\text{CH}_2\text{O}$), 57.01 ($\text{MeC}(\text{Ox}^{\text{Me}_2})_2$), 30.04 ($\text{CNCMe}_2\text{CH}_2\text{O}$), 12.41 ($\text{MeC}(\text{Ox}^{\text{Me}_2})_2$). $^{15}\text{N}\{^1\text{H}\}$ NMR (THF- d_8 , 61 MHz): δ -211.3 ($\text{CNCMe}_2\text{CH}_2\text{O}$). IR (KBr, cm^{-1}): 2964 s, 2928 m, 2867 m, 1671 w, 1615 s, 1590 s, 1543 m, 1509 s, 1460 m, 1397 m, 1361 m, 1293 m, 1245 w, 1189 m, 1070 m, 1019 s, 980 m, 922 w, 828 w, 767 w, 732 w. Anal. Calcd for $\text{C}_{12}\text{H}_{19}\text{LiN}_2\text{O}_2$: C, 62.6; H, 8.32; N, 12.17. Found: C, 62.29; H, 8.55; N, 12.06.

$\text{Bo}^{\text{M}}\text{CpH}$. $\text{Ti}[\text{C}_5\text{H}_5]_3$ (1.44 g, 5.35 mmol) was slurried in benzene (10 mL) in a 100 mL Schlenk flask. The flask was fitted with an addition funnel, and the solution was cooled to 12 °C using a dioxane/dry ice bath. A solution of iodine (1.24 g, 4.86 mmol) in benzene (50 mL) was added to the slurry in a dropwise fashion over 1.5 h while maintaining the temperature at 12 °C to form a cloudy yellow solution of $\text{C}_5\text{H}_5\text{I}$. $\text{MeC}(\text{Ox}^{\text{Me}_2})_2\text{Li}$ (1.12 g, 4.86 mmol) dissolved in THF (20 mL) was added to the iodocyclopentadiene mixture via cannula. The solution was then warmed to room temperature and stirred overnight. The solution was filtered in air, and the solvent was evaporated on a Rotovapor at 100 mTorr. The crude oily product was purified by silica gel chromatography in ethyl acetate to give a brown oil, which was dissolved in benzene and stirred over phosphorus pentoxide for 6 h to remove any water. The solution was filtered and the solvent was removed under reduced pressure to provide brown, oily $\text{Bo}^{\text{M}}\text{CpH}$ as a mixture of two isomers (0.789 g, 2.753 mmol, 57%). ^1H NMR (benzene- d_6 , 600 MHz): δ 7.04 (m, 1 H, $\text{H}_2\text{C}_5\text{H}_3$), 6.58 (s, 1 H, $\text{H}_2\text{C}_5\text{H}_3$), 6.41 (m, 1 H, $\text{H}_2\text{C}_5\text{H}_3$), 6.35 (m, 2 H, $\text{H}_2\text{C}_5\text{H}_3$), 6.31 (m, 1 H, $\text{H}_2\text{C}_5\text{H}_3$), 3.66–3.58 (m, 8 H, $\text{CNCMe}_2\text{CH}_2\text{O}$), 3.46 (s, 2 H, $\text{H}_2\text{C}_5\text{H}_3$), 2.73 (s, 2 H, $\text{H}_2\text{C}_5\text{H}_3$), 2.10 (s, 3 H, $\text{MeC}(\text{Ox}^{\text{Me}_2})_2$), 2.04 (s, 3 H, $\text{MeC}(\text{Ox}^{\text{Me}_2})_2$), 1.11 (v t, 24 H, $\text{CNCMe}_2\text{CH}_2\text{O}$). $^{13}\text{C}\{^1\text{H}\}$ NMR (benzene- d_6 , 151 MHz): δ 166.56 ($\text{CNCMe}_2\text{CH}_2\text{O}$), 166.23 ($\text{CNCMe}_2\text{CH}_2\text{O}$), 148.24 ($\text{H}_2\text{C}_5\text{H}_3$), 147.17 ($\text{H}_2\text{C}_5\text{H}_3$), 135.26 ($\text{H}_2\text{C}_5\text{H}_3$), 133.46 ($\text{H}_2\text{C}_5\text{H}_3$), 132.55 ($\text{H}_2\text{C}_5\text{H}_3$), 132.18 ($\text{H}_2\text{C}_5\text{H}_3$), 129.60 ($\text{H}_2\text{C}_5\text{H}_3$), 128.92 ($\text{H}_2\text{C}_5\text{H}_3$), 79.55 ($\text{CNCMe}_2\text{CH}_2\text{O}$), 79.53 ($\text{CNCMe}_2\text{CH}_2\text{O}$), 67.72 ($\text{CNCMe}_2\text{CH}_2\text{O}$), 67.66 ($\text{CNCMe}_2\text{CH}_2\text{O}$), 45.31 ($\text{H}_2\text{C}_5\text{H}_3$), 44.68 ($\text{H}_2\text{C}_5\text{H}_3$), 43.21 ($\text{MeC}(\text{Ox}^{\text{Me}_2})_2$), 41.42 ($\text{MeC}(\text{Ox}^{\text{Me}_2})_2$), 28.60 ($\text{CNCMe}_2\text{CH}_2\text{O}$), 28.55 ($\text{CNCMe}_2\text{CH}_2\text{O}$), 28.51 ($\text{CNCMe}_2\text{CH}_2\text{O}$), 24.48 ($\text{MeC}(\text{Ox}^{\text{Me}_2})_2$), 23.83 ($\text{MeC}(\text{Ox}^{\text{Me}_2})_2$). ^{15}N NMR (benzene- d_6 , 61 MHz): δ -132.5 ($\text{CNCMe}_2\text{CH}_2\text{O}$). IR (KBr, cm^{-1}): 2968 s, 2930 m, 2890 m, 1656 s ($\text{C}=\text{N}$), 1462 m, 1364 m, 1286 m, 1249 w, 1193 m, 1084 m, 974 m, 933 w, 900 w, 732 w. Anal. Calcd for $\text{C}_{17}\text{H}_{24}\text{N}_2\text{O}_2$: C, 70.80; H, 8.39; N, 9.71. Found: C, 70.30; H, 8.78; N, 9.69.

$\text{Bo}^{\text{M}}\text{CpTI}$. $\text{Bo}^{\text{M}}\text{CpH}$ (0.375 g, 1.31 mmol) was dissolved in diethyl ether. Thallium ethoxide (102 μL , 1.44 mmol) was added, and a brown precipitate immediately formed. The solution was stirred at room temperature for 2 h. The mixture was centrifuged, and the solvent was decanted. The solid was washed with pentane (3 \times) and

was then extracted with benzene, filtered, and dried under reduced pressure to give the product as a brown solid (0.537 g, 1.09 mmol, 83%). Mp: 168–171 °C (dec). ^1H NMR (benzene- d_6 , 600 MHz): δ 6.56 (s, 2 H, C_5H_4), 6.29 (s, 2 H, C_5H_4), 3.65 (d, 2 H, $^2J_{\text{HH}} = 8$ Hz, $\text{CNCMe}_2\text{CH}_2\text{O}$), 3.59 (d, 2 H, $^2J_{\text{HH}} = 8$ Hz, $\text{CNCMe}_2\text{CH}_2\text{O}$), 2.14 (s, 3 H, $\text{MeC}(\text{Ox}^{\text{Me}_2})_2$), 1.03 (s, 6 H, $\text{CNCMe}_2\text{CH}_2\text{O}$), 1.01 (s, 6 H, $\text{CNCMe}_2\text{CH}_2\text{O}$). $^{13}\text{C}\{^1\text{H}\}$ NMR (benzene- d_6 , 151 MHz): δ 170.92 ($\text{CNCMe}_2\text{CH}_2\text{O}$), 124.22 (C_5H_4), 107.90 (C_5H_4), 107.52 (C_5H_4), 80.14 ($\text{CNCMe}_2\text{CH}_2\text{O}$), 67.31 ($\text{CNCMe}_2\text{CH}_2\text{O}$), 44.21 ($\text{MeC}(\text{Ox}^{\text{Me}_2})_2$), 28.46 ($\text{CNCMe}_2\text{CH}_2\text{O}$), 28.39 ($\text{CNCMe}_2\text{CH}_2\text{O}$), 25.17 ($\text{MeC}(\text{Ox}^{\text{Me}_2})_2$). ^{15}N NMR (benzene- d_6 , 61 MHz): δ -130 ($\text{CNCMe}_2\text{CH}_2\text{O}$). IR (KBr, cm^{-1}): 3075 m, 2966 s, 2930 m, 2887 s, 1647 s ($\text{C}=\text{N}$), 1463 m, 1383 w, 1365 m, 1349 w, 1276 m, 1248 m, 1200 m, 1080 s, 1042 vw, 1028 w, 975 m. Anal. Calcd for $\text{C}_{17}\text{H}_{23}\text{N}_2\text{O}_2\text{Ti}$: C, 41.52; H, 4.71; N, 5.70. Found: C, 41.14; H, 4.61; N, 5.67.

$\text{Bo}^{\text{M}}\text{Cp}^{\text{tetH}}$. TIOEt (84.9 μL , 1.20 mmol) was added to a THF solution of $\text{Bo}^{\text{M}}\text{Cp}^{\text{tetH}}$ (0.377 g, 1.09 mmol), and the reaction mixture was stirred at room temperature for 10 days. The volatile materials were evaporated, and the solid was washed with pentane (3 \times). The residue was extracted with benzene and dried under reduced pressure to give the product as a green solid (0.512 g, 0.933 mmol, 85.5%). Mp: 162–164 °C (dec). ^1H NMR (benzene- d_6 , 600 MHz): δ 3.65 (d, $^2J_{\text{HH}} = 8.1$ Hz, 2 H, $\text{CNCMe}_2\text{CH}_2\text{O}$), 3.63 (d, $^2J_{\text{HH}} = 8.1$ Hz, 2 H, $\text{CNCMe}_2\text{CH}_2\text{O}$), 2.36 (s, 6 H, C_5Me_4), 2.24 (s, 6 H, C_5Me_4), 2.20 (s, 3 H, $\text{MeC}(\text{Ox}^{\text{Me}_2})_2$), 1.11 (s, 6 H, $\text{CNCMe}_2\text{CH}_2\text{O}$), 1.10 (s, 6 H, $\text{CNCMe}_2\text{CH}_2\text{O}$). $^{13}\text{C}\{^1\text{H}\}$ NMR (benzene- d_6 , 151 MHz): δ 170.23 ($\text{CNCMe}_2\text{CH}_2\text{O}$), 115.94 (C_5Me_4), 114.8 (C_5Me_4), 114.1 (br, C_5Me_4), 79.83 ($\text{CNCMe}_2\text{CH}_2\text{O}$), 67.62 ($\text{CNCMe}_2\text{CH}_2\text{O}$), 46.53 ($\text{MeC}(\text{Ox}^{\text{Me}_2})_2$), 28.76 ($\text{CNCMe}_2\text{CH}_2\text{O}$), 28.26 ($\text{CNCMe}_2\text{CH}_2\text{O}$), 26.65 ($\text{MeC}(\text{Ox}^{\text{Me}_2})_2$), 12.63 (d, $J_{\text{TIC}} = 57.4$ Hz, C_5Me_4), 11.14 (d, $J_{\text{TIC}} = 44.8$ Hz, C_5Me_4). ^{15}N NMR (benzene- d_6 , 61 MHz): δ -128.1 ($\text{CNCMe}_2\text{CH}_2\text{O}$). IR (KBr, cm^{-1}): 2971 s, 2961 m, 2923 m, 2889 m, 2855 m, 1654 m ($\text{C}=\text{N}$), 1637 s ($\text{C}=\text{N}$), 1457 w, 1381 m, 1362 w, 1343 w, 1267 m, 1246 m, 1194 m, 1091 m, 1075 m, 1042 w, 993 m, 973 m, 936 w, 897 w. Anal. Calcd for $\text{C}_{21}\text{H}_{31}\text{N}_2\text{O}_2\text{Ti}$: C, 46.04; H, 5.70; N, 5.11. Found: C, 46.21; H, 5.79; N, 5.06.

$\{\text{Bo}^{\text{M}}\text{Cp}\}\text{MgMe}$. $\text{MgMe}_2(\text{O}_2\text{C}_4\text{H}_8)_2$ (0.049 g, 0.230 mmol) was added to a benzene solution of $\text{Bo}^{\text{M}}\text{CpH}$ (0.066 g, 0.230 mmol), and the reaction mixture was stirred at room temperature for 1.5 h. Gas formation was observed over the course of the reaction. The solution was filtered, and the filtrate was evaporated under reduced pressure to give a pink oil. The oil was washed with pentane (3 \times) and dried under reduced pressure to give a white solid, which was stored at -30 °C (0.051 g, 0.157 mmol, 68.3%). Exhaustive evaporation to remove residual dioxane and diethyl ether gives broad spectra. Data given here contain residual ethers, the 2C and magnesium methyl signals were not detected in the $^{13}\text{C}\{^1\text{H}\}$ NMR spectrum or through 2D correlation spectroscopy, and C analyses were systematically lower than calculated values. Mp: 145–147 °C (dec). ^1H NMR (benzene- d_6 , 600 MHz): δ 6.44 (s, 2 H, C_5H_4), 6.33 (s, 2 H, C_5H_4), 3.66 (d, 2 H, $^2J_{\text{HH}} = 8.1$ Hz, $\text{CNCMe}_2\text{CH}_2\text{O}$), 3.55 (d, 2 H, $^2J_{\text{HH}} = 8.1$ Hz, $\text{CNCMe}_2\text{CH}_2\text{O}$), 2.06 (s, 3 H, $\text{MeC}(\text{Ox}^{\text{Me}_2})_2$), 1.16 (6 H, $\text{CNCMe}_2\text{CH}_2\text{O}$), 1.13 (6 H, $\text{CNCMe}_2\text{CH}_2\text{O}$), -0.05 (br s, MgMe). $^{13}\text{C}\{^1\text{H}\}$ NMR (benzene- d_6 , 151 MHz): δ 118.46 (C_5H_4), 108.54 (C_5H_4), 102.46 (C_5H_4), 81.16 ($\text{CNCMe}_2\text{CH}_2\text{O}$), 66.94 ($\text{CNCMe}_2\text{CH}_2\text{O}$), 44.89 ($\text{MeC}(\text{Ox}^{\text{Me}_2})_2$), 28.29 ($\text{CNCMe}_2\text{CH}_2\text{O}$), 28.22 ($\text{CNCMe}_2\text{CH}_2\text{O}$), 22.20 ($\text{MeC}(\text{Ox}^{\text{Me}_2})_2$). ^{15}N NMR (benzene- d_6 , 61 MHz): δ -147.4 ($\text{CNCMe}_2\text{CH}_2\text{O}$). IR (KBr, cm^{-1}): 2968 s, 2931 m, 2897 m, 1658 s ($\text{C}=\text{N}$), 1547 w, 1463 m, 1366 m, 1309 w, 1292 w, 1255 w, 1202 w, 1192 m, 1084 s sh, 1041 s, 974 w, 960 w, 934 w, 874 m, 809 w, 750 m. Anal. Calcd for $\text{C}_{18}\text{H}_{26}\text{MgN}_2\text{O}_2$: C, 66.17; H, 8.02; N, 8.57. Found: C, 63.34; H, 7.61; N, 8.67.

$\{\text{Bo}^{\text{M}}\text{Cp}^{\text{tetH}}\}\text{MgMe}$. A benzene solution of $\text{Bo}^{\text{M}}\text{Cp}^{\text{tetH}}$ (0.129 g, 0.373 mmol) was allowed to react with $\text{MgMe}_2(\text{O}_2\text{C}_4\text{H}_8)_2$ (0.080 g, 0.373 mmol) at room temperature for 4 h. Gas formation was observed over the course of the reaction. The reaction mixture was filtered and evaporated to dryness under reduced pressure to give a yellow oil. The oil was washed with pentane (3 \times) and dried under reduced pressure to give a white solid, which was stored at -30 °C

(0.110 g, 0.286 mmol, 76.9%). Mp: 145–146 °C (dec). ^1H NMR (benzene- d_6 , 600 MHz): δ 3.70 (d, 2 H, $^2J = 8.3$ Hz, $\text{CNCMe}_2\text{CH}_2\text{O}$), 3.58 (d, 2 H, $^2J = 8.3$ Hz, $\text{CNCMe}_2\text{CH}_2\text{O}$), 2.33 (s, 6 H, C_5Me_4), 2.24 (s, 6 H, C_5Me_4), 2.11 (s, 3 H, $\text{MeC}(\text{Ox}^{\text{Me}_2})_2$), 1.08 (s, 6 H, $\text{CNCMe}_2\text{CH}_2\text{O}$), 1.05 (s, 6 H, $\text{CNCMe}_2\text{CH}_2\text{O}$), -0.91 (s, 3 H, MgMe). $^{13}\text{C}\{^1\text{H}\}$ NMR (benzene- d_6 , 151 MHz): δ 173.8 ($\text{CNCMe}_2\text{CH}_2\text{O}$), 113.66 (C_5Me_4), 108.19 (C_5Me_4), 107.47 (C_5Me_4), 80.81 ($\text{CNCMe}_2\text{CH}_2\text{O}$), 66.51 ($\text{CNCMe}_2\text{CH}_2\text{O}$), 46.69 ($\text{MeC}(\text{Ox}^{\text{Me}_2})_2$), 28.61 ($\text{CNCMe}_2\text{CH}_2\text{O}$), 27.73 ($\text{CNCMe}_2\text{CH}_2\text{O}$), 24.11 ($\text{MeC}(\text{Ox}^{\text{Me}_2})_2$), 14.01 (C_5Me_4), 11.97 (C_5Me_4), -10.84 (MgMe). ^{15}N NMR (benzene- d_6 , 61 MHz): δ -145.7 ($\text{CNCMe}_2\text{CH}_2\text{O}$). IR (KBr, cm^{-1} , amorphous solid): 2996 s, 2928 s, 2866 s, 2726 w sh, 1658 s (C=N), 1496 m, 1467 m, 1304 m, 1306 m, 1283 m, 1252 m, 1192 m, 1087 m, 1024 w, 991 w, 974 m, 962 m, 934 m, 893 w, 829 w. IR (crystallized sample, KBr, cm^{-1}): 2966 s, 2928 s, 2897 s, 2867 s, 1657 s, 1627 s, 1462 m, 1365 m, 1307 m, 1253 w, 1190 m, 1088 s, 1024 w, 961 m, 935 m, 831 w. Anal. Calcd for $\text{C}_{22}\text{H}_{34}\text{MgN}_2\text{O}_2$: C, 69.02; H, 8.95; N, 7.32. Found: C, 67.48; H, 9.35; N, 6.95.

$\{[\text{Bo}^{\text{M}}\text{Cp}]\text{TiCl}(\mu\text{-Cl})\}_2$. $\text{TiCl}_3(\text{THF})_3$ (0.194 g, 0.523 mmol) was dissolved in benzene (10 mL) and added to a benzene solution of $\text{Bo}^{\text{M}}\text{CpTi}$ (0.257 g, 0.523 mmol) to produce a cloudy green solution. The reaction mixture was stirred for 8 h. The solution was filtered, and the filtrate was evaporated to dryness under reduced pressure to give a brown solid. The solid was recrystallized at -30 °C in a mixture of toluene and pentane to give green, paramagnetic X-ray quality crystals (0.113 g, 0.278 mmol, 53.1%). Mp: 140–142 °C (dec). IR (KBr, cm^{-1}): 3117 w, 2970 m, 1662 s (C=N), 1635 s (C=N), 1461 m, 1368 s, 1323 s, 1290 m, 1258 m, 1190 m, 1109 s, 1090 s, 1050 w, 1036 w, 982 s, 960 s, 935 m, 874 w, 822 s, 808 s, 773 w. Anal. Calcd for $\text{C}_{17}\text{H}_{23}\text{Cl}_2\text{N}_2\text{O}_2\text{Ti}$: C, 50.27; H, 5.71; N, 6.90. Found: C, 49.92; H, 5.64; N, 6.84.

Magnetic susceptibility was measured using Evan's method at room temperature using a Bruker 400 MHz NMR spectrometer. A sample of $\text{Bo}^{\text{M}}\text{CpTiCl}_2$ (5.7 mg, 0.014 mmol) was dissolved in benzene- d_6 (0.90 mL) to give a 15.6 mM solution. The solution (0.60 mL) was placed in an NMR tube. A capillary was charged with benzene- d_6 and placed in the NMR tube. The ^1H NMR spectrum showed a paramagnetic shift in the benzene- d_6 peak. Using Evan's method, the following values were obtained: $\Delta\delta = 0.070$ ppm, $\chi_{\text{mol}} = 1.07 \times 10^{-3}$ cm^3/mol , $\mu = 1.60$ μ_{B} , $n = 0.885$ electron. The data are consistent with a d^1 Ti(III) complex.

$\{[\text{Bo}^{\text{M}}\text{Cp}^{\text{tet}}]\text{TiCl}(\mu\text{-Cl})\}_2$. $\text{TiCl}_3(\text{THF})_3$ (0.071 g, 0.192 mmol) was dissolved in benzene (5 mL) and added to a benzene solution of $\text{Bo}^{\text{M}}\text{Cp}^{\text{tet}}\text{Ti}$ (0.257 g, 0.523 mmol), resulting in a cloudy green solution. The reaction mixture was stirred for 18 h. The solution was filtered, and the filtrate was evaporated to dryness under reduced pressure. The solid was then extracted with benzene and dried under reduced pressure to give a green solid (0.070 g, 0.151 mmol, 79%). Mp: 141–143 °C (dec). IR (KBr, cm^{-1}): 2964 s, 2927 m, 2871 w, 1661 m sh (C=N), 1641 s (C=N), 1570 w, 1463 m, 1366 m, 1322 m, 1285 w, 1253 w, 1190 m, 1170 m, 1096 m, 1029 w, 973 m, 956 m, 935 w, 832 w. $n = 0.69$ by Evan's method. Anal. Calcd for $\text{C}_{21}\text{H}_{31}\text{Cl}_2\text{N}_2\text{O}_2\text{Ti}$: C, 54.56; H, 6.76; N, 6.06. Found: C, 53.82; H, 6.75; N, 5.84.

$\{\text{Bo}^{\text{M}}\text{Cp}\}\text{Zr}(\text{NMe}_2)_3$. Benzene solutions of $\text{Bo}^{\text{M}}\text{CpH}$ (0.100 g, 0.347 mmol) and $\text{Zr}(\text{NMe}_2)_4$ (0.093 g, 0.347 mmol) were mixed, allowed to stir for 1 h at room temperature, and then filtered. Evaporation of the filtrate to dryness under reduced pressure provided a yellow gel, which was washed with pentane (3×5 mL). Further drying under vacuum yielded $\{\text{Bo}^{\text{M}}\text{Cp}\}\text{Zr}(\text{NMe}_2)_3$ as a yellow, analytically pure solid (0.168 g, 0.329 mmol, 94.9%). X-ray quality single crystals were obtained from a toluene and pentane solution of the product at -30 °C. Mp: 129–132 °C. ^1H NMR (benzene- d_6 , 600 MHz): δ 6.24 (t, 2 H, $^3J_{\text{HH}} = 2.2$ Hz, C_5H_4), 6.20 (t, 2 H, $^3J_{\text{HH}} = 2.2$ Hz, C_5H_4), 3.63 (d, 2 H, $^2J_{\text{HH}} = 8.1$ Hz, $\text{CNCMe}_2\text{CH}_2\text{O}$), 3.52 (d, 2 H, $^2J_{\text{HH}} = 8.1$ Hz, $\text{CNCMe}_2\text{CH}_2\text{O}$), 3.09 (s, 18 H, NMe_2), 1.92 (s, 3 H, $\text{MeC}(\text{Ox}^{\text{Me}_2})_2$), 1.02 (s, 6 H, $\text{CNCMe}_2\text{CH}_2\text{O}$), 0.97 (s, 6 H, $\text{CNCMe}_2\text{CH}_2\text{O}$). $^{13}\text{C}\{^1\text{H}\}$ NMR (151 MHz, benzene- d_6): δ 170.42 ($\text{CNCMe}_2\text{CH}_2\text{O}$), 126.30 (*ipso*- C_5H_4), 109.36 (C_5H_4), 108.98 (C_5H_4), 80.73 ($\text{CNCMe}_2\text{CH}_2\text{O}$),

67.81 ($\text{CNCMe}_2\text{CH}_2\text{O}$), 47.36 (NMe_2), 43.92 ($\text{MeC}(\text{Ox}^{\text{Me}_2})_2$), 27.33 ($\text{CNCMe}_2\text{CH}_2\text{O}$), 27.03 ($\text{CNCMe}_2\text{CH}_2\text{O}$), 22.42 ($\text{MeC}(\text{Ox}^{\text{Me}_2})_2$). ^{15}N NMR (benzene- d_6 , 61 MHz): δ -138 ($\text{CNCMe}_2\text{CH}_2\text{O}$); $\text{Zr}(\text{NMe}_2)_3$ was not detected. IR (KBr, cm^{-1} , amorphous solid): 2965 s, 2930 m, 2890 m, 2865 m, 2819 m, 2759 m, 2736 m, 1645 s (C=N), 1460 m, 1364 m, 1314 m, 1288 m, 1235 m, 1203 m, 1139 s, 1122 m, 1102 m, 1083 m, 1046 s, 975 s, 957 m, 938 m, 875 m, 786 s, 715 m, 712 s. Anal. Calcd for $\text{C}_{23}\text{H}_{41}\text{N}_5\text{O}_2\text{Zr}$: C, 54.08; H, 8.09; N, 13.71. Found: C, 53.63; H, 7.57; N, 13.30.

General Procedure for Catalytic Hydroamination. *Micro-molar-Scale Catalysis.* In a typical small-scale hydroamination experiment, a J. Young style NMR tube was charged with 100 μmol of aminoalkene substrate, 10 μmol of catalyst, and 0.5 mL of solvent (benzene- d_6). The J. Young tube was sealed with a Teflon valve, and the reaction progress was monitored by ^1H NMR spectroscopy at regular intervals to determine the conversion.

Scaled-Up Hydroamination Catalysis. A Schlenk flask was charged with the catalyst $\{\text{Bo}^{\text{M}}\text{Cp}\}\text{MX}$ or $\{\text{Bo}^{\text{M}}\text{Cp}^{\text{tet}}\}\text{MX}$ (0.200 mmol), the appropriate aminoalkene (2.00 mmol), and benzene (10 mL). The solution was stirred for 4 to 48 h at room temperature. The products were isolated by evaporation of the solvent and purified using flash column chromatography (silica gel, $\text{CH}_2\text{Cl}_2/\text{MeOH} = 9.5:0.5$).

■ ASSOCIATED CONTENT

📄 Supporting Information

The Supporting Information is available free of charge on the ACS Publications website at DOI: 10.1021/acs.organomet.5b00771.

^1H , $^{13}\text{C}\{^1\text{H}\}$, and ^{15}N NMR spectra of new compounds (PDF)

Crystallographic information files for $\text{Bo}^{\text{M}}\text{Cp}^{\text{tet}}\text{H}$, $\{\text{Bo}^{\text{M}}\text{Cp}^{\text{tet}}\}\text{MgMe}$, $\{\text{Bo}^{\text{M}}\text{Cp}\}\text{TiCl}_2$, and $\{\text{Bo}^{\text{M}}\text{Cp}\}\text{Zr}(\text{NMe}_2)_3$ (CIF)

■ AUTHOR INFORMATION

Corresponding Author

*E-mail: sadow@iastate.edu.

Present Addresses

Megan Hovey, Oxbow Carbon LLC, 11826 N 30th Street, Kremlin, Oklahoma 73753, United States.

Hung-An Ho, Catal Material Co. Ltd., 33 Guangfu Road, Jiatai Industrial Park, Chiayi, Taiwan 61252.

Barun Jana, Department of Inorganic Chemistry, Indian Association for the Cultivation of Science, Kolkata, 700032 India.

Nicole L. Lampland, Pharmaceutical Speciality, Inc. 1620 Industrial Drive NW, Rochester, Minnesota 55901, United States.

Notes

The authors declare no competing financial interest.

■ ACKNOWLEDGMENTS

Drs. Sarah Cady and Toshia Zessin are thanked for valuable assistance with EPR spectra measurements and analysis. This research was supported by the U.S. Department of Energy, Office of Basic Energy Sciences, Division of Chemical Sciences, Geosciences, and Biosciences, through the Ames Laboratory Catalysis Program (Contract No. DE-AC02-07CH11358). M.H. was supported by Office of Workforce Development for Teachers and Scientists through the Summer Undergraduate Laboratory Internship Program through the Ames Laboratory.

REFERENCES

- (1) (a) Fryzuk, M. D.; Mao, S. S. H.; Zaworotko, M. J.; MacGillivray, L. R. *J. Am. Chem. Soc.* **1993**, *115*, 5336–7. (b) Hirotsu, M.; Fontaine, P. P.; Epshteyn, A.; Sita, L. R. *J. Am. Chem. Soc.* **2007**, *129*, 9284–9285. (c) Hirotsu, M.; Fontaine, P. P.; Zavalij, P. Y.; Sita, L. R. *J. Am. Chem. Soc.* **2007**, *129*, 12690–12692. (d) Shima, T.; Hu, S.; Luo, G.; Kang, X.; Luo, Y.; Hou, Z. *Science* **2013**, *340*, 1549–1552.
- (2) (a) Arndt, S.; Okuda, J. *Chem. Rev.* **2002**, *102*, 1953–1976. (b) Gibson, V. C.; Spitzmesser, S. K. *Chem. Rev.* **2002**, *103*, 283–316.
- (3) (a) Okuda, J. *Chem. Ber.* **1990**, *123*, 1649–1651. (b) Shapiro, P. J.; Bunel, E.; Schaefer, W. P.; Bercaw, J. E. *Organometallics* **1990**, *9*, 867–869. (c) Stevens, J. C. *InsiteTM Catalysts Structure/Activity Relationships for Olefin Polymerization*. In *Catalyst Design for Tailor-Made Polyolefins: Proceedings of the International Symposium on Catalyst Design for Tailor-Made Polyolefins*; Kanazawa, March 10–12, 1994; Soga, K.; Terano, M., Eds.; Elsevier: Tokyo, 1994; Vol. 89, pp 277–284. (d) Chen, Y.-X.; Marks, T. J. *Organometallics* **1997**, *16*, 3649–3657.
- (4) (a) Manna, K.; Ellern, A.; Sadow, A. D. *Chem. Commun.* **2010**, *46*, 339–341. (b) Manna, K.; Kruse, M. L.; Sadow, A. D. *ACS Catal.* **2011**, *1*, 1637–1642. (c) Manna, K.; Xu, S.; Sadow, A. D. *Angew. Chem., Int. Ed.* **2011**, *50*, 1865–1868. (d) Manna, K.; Everett, W. C.; Schoendorff, G.; Ellern, A.; Windus, T. L.; Sadow, A. D. *J. Am. Chem. Soc.* **2013**, *135*, 7235–7250.
- (5) Stubbert, B. D.; Marks, T. J. *J. Am. Chem. Soc.* **2007**, *129*, 6149–6167.
- (6) Tian, S.; Arredondo, V. M.; Stern, C. L.; Marks, T. J. *Organometallics* **1999**, *18*, 2568–2570.
- (7) (a) Hangaly, N. K.; Petrov, A. R.; Rufanov, K. A.; Harms, K.; Elfferding, M.; Sundermeyer, J. *Organometallics* **2011**, *30*, 4544–4554. (b) Otero, A.; Lara-Sánchez, A.; Nájera, C.; Fernández-Baeza, J.; Márquez-Segovia, I.; Castro-Osma, J. A.; Martínez, J.; Sánchez-Barba, L. F.; Rodríguez, A. M. *Organometallics* **2012**, *31*, 2244–2255.
- (8) Bertolasi, V.; Boaretto, R.; Chierotti, M. R.; Gobetto, R.; Sostero, S. *Dalton Trans.* **2007**, 5179–5189.
- (9) Rufanov, K. A.; Petrov, A. R.; Kotov, V. V.; Laquai, F.; Sundermeyer, J. *Eur. J. Inorg. Chem.* **2005**, 3805–3807.
- (10) (a) Otero, A.; Fernandez-Baeza, J.; Antinolo, A.; Tejada, J.; Lara-Sanchez, A.; Sanchez-Barba, L.; Rodriguez, A. M.; Maestro, M. A. *J. Am. Chem. Soc.* **2004**, *126*, 1330–1331. (b) Otero, A.; Fernandez-Baeza, J.; Antinolo, A.; Tejada, J.; Lara-Sanchez, A.; Sanchez-Barba, L. F.; Sanchez-Molina, M.; Rodriguez, A. M.; Bo, C.; Urbano-Cuadrado, M. *Organometallics* **2007**, *26*, 4310–4320.
- (11) Breslow, R.; Canary, J. W. *J. Am. Chem. Soc.* **1991**, *113*, 3950–3952.
- (12) (a) Gade, L. H.; Bellemin-Lapponnaz, S. *Chem. - Eur. J.* **2008**, *14*, 4142–4152. (b) Bellemin-Lapponnaz, S.; Gade, L. H. *Chem. Commun.* **2002**, 1286–1287.
- (13) Liao, S.; Sun, X.-L.; Tang, Y. *Acc. Chem. Res.* **2014**, *47*, 2260–2272.
- (14) Lampland, N. L.; Zhu, J.; Hovey, M.; Jana, B.; Ellern, A.; Sadow, A. D. *Inorg. Chem.* **2015**, *54*, 6938–6946.
- (15) Bauer, A.; Hilbig, H.; Hiller, W.; Hinterschwepfinger, E.; Köhler, F. H.; Neumayer, M. *Synthesis* **2001**, 778–782.
- (16) Werner, H.; Otto, H.; Kraus, H. J. *J. Organomet. Chem.* **1986**, *315*, C57–C60.
- (17) Pawlikowski, A. V.; Gray, T. S.; Schoendorff, G.; Baird, B.; Ellern, A.; Windus, T. L.; Sadow, A. D. *Inorg. Chim. Acta* **2009**, *362*, 4517–4525.
- (18) (a) Dunne, J. F.; Fulton, D. B.; Ellern, A.; Sadow, A. D. *J. Am. Chem. Soc.* **2010**, *132*, 17680–17683. (b) Mukherjee, D.; Ellern, A.; Sadow, A. D. *Chem. Sci.* **2014**, *5*, 959–964. (c) Sibi, M. P.; Shay, J. J.; Liu, M.; Jasperse, C. P. *J. Am. Chem. Soc.* **1998**, *120*, 6615–6616.
- (19) Westerhausen, M.; Makropoulos, N.; Wieneke, B.; Karaghiosoff, K.; Nöth, H.; Schwenk-Kircher, H.; Knizek, J.; Seifert, T. *Eur. J. Inorg. Chem.* **1998**, 965–971.
- (20) Garcés, A.; Sánchez-Barba, L. F.; Alonso-Moreno, C.; Fajardo, M.; Fernández-Baeza, J.; Otero, A.; Lara-Sánchez, A.; López-Solera, I.; Rodríguez, A. M. *Inorg. Chem.* **2010**, *49*, 2859–2871.
- (21) Jaenschke, A.; Paap, J.; Behrens, U. *Organometallics* **2003**, *22*, 1167–1169.
- (22) Mukherjee, D.; Lampland, N. L.; Yan, K.; Dunne, J. F.; Ellern, A.; Sadow, A. D. *Chem. Commun.* **2013**, *49*, 4334–4336.
- (23) Pattiasina, J. W.; Heeres, H. J.; Van Bolhuis, F.; Meetsma, A.; Teuben, J. H.; Spek, A. L. *Organometallics* **1987**, *6*, 1004–1010.
- (24) Samuel, E.; Harrod, J. F.; Gourier, D.; Dromzee, Y.; Robert, F.; Jeannin, Y. *Inorg. Chem.* **1992**, *31*, 3252–3259.
- (25) Jungst, R.; Sekutowski, D.; Davis, J.; Luly, M.; Stucky, G. *Inorg. Chem.* **1977**, *16*, 1645–1655.
- (26) Dunne, J. F.; Su, J.; Ellern, A.; Sadow, A. D. *Organometallics* **2008**, *27*, 2399–2401.
- (27) Dagonne, S.; Bellemin-Lapponnaz, S.; Welter, R. *Organometallics* **2004**, *23*, 3053–3061.
- (28) Tobia, D.; Baranski, J.; Rickborn, B. J. *Org. Chem.* **1989**, *54*, 4253–4256.
- (29) Diamond, G. M.; Jordan, R. F.; Petersen, J. L. *J. Am. Chem. Soc.* **1996**, *118*, 8024–8033.
- (30) Corey, E. J.; Koelliker, U.; Neuffer, J. *J. Am. Chem. Soc.* **1971**, *93*, 1489–1490.
- (31) Fendrick, C. M.; Schertz, L. D.; Day, V. W.; Marks, T. J. *Organometallics* **1988**, *7*, 1828–1838.
- (32) Hong, S.; Tian, S.; Metz, M. V.; Marks, T. J. *J. Am. Chem. Soc.* **2003**, *125*, 14768–83.
- (33) Bender, C. F.; Widenhoefer, R. A. *J. Am. Chem. Soc.* **2005**, *127*, 1070–1071.
- (34) Riegert, D.; Collin, J.; Meddour, A.; Schulz, E.; Trifonov, A. J. *Org. Chem.* **2006**, *71*, 2514–2517.